Photochemical Reaction Dynamics of 2,2'-Dithiobis(Benzothiazole): Direct Observation of the Addition Product of an Aromatic Thiyl Radical to an Alkene with Time-Resolved Vibrational and Electronic Absorption Spectroscopy

Daisuke Koyama, and Andrew J. Orr-Ewing*

School of Chemistry, University of Bristol, Cantock's Close, Bristol BS8 1TS, UK

15 April 2016

* Author for Correspondence

Tel: +44 (0)117 9287672

e-mail: A.Orr-Ewing@bristol.ac.uk

KEYWORDS: Time-Resolved Absorption Spectroscopy; Photolysis of Aromatic Disulfide; Thiol-Ene Reaction; Reaction Rates.

ABSTRACT

The photochemical reaction dynamics of the benzothiazole-2-thiyl (BS) radical, produced by 330 nm ultraviolet photolysis of 2,2'-dithiobis(benzothiazole) (BSSB), are examined on the picosecond time scale. The initial addition product of a thiol-ene reaction between the BS radical and styrene is directly observed by transient vibrational absorption spectroscopy (TVAS). Transient electronic absorption spectroscopy (TEAS) in the ultraviolet and visible spectral regions reveals rapid formation of the ground state BS radical with a time constant of ~200 fs. The photolytically generated BS radical decays through geminate recombination to the parent molecule BSSB and competitive formation of a BS radical dimer with a rate coefficient of $(3.7 \pm 0.2) \times 10^{10}$ M^{-1} s^{-1} in methanol, and thereafter (36 ± 1) % of the initially formed BS radicals survive at the longest time delay (1.3 ns). In styrene solution, in contrast to methanol and toluene solutions, kinetic traces of the BS radical show an additional decay with a time constant of 305 ± 13 ps, and a broad band at 345 − 500 nm grows with the same time constant, suggesting a bimolecular reaction of the BS radical with styrene. The TVAS measurements reveal an absorption band of the ground state BS radical at 1301 cm^{-1} in toluene solution, and the band decays with a time constant of 294 ± 32 ps in styrene solution. Two product bands grow at 1239 cm^{-1} and 1429 cm^{-1} with respective time constants of 312 ± 68 ps and 325 ± 33 ps, and are attributed to the addition product BS-St radical formed from the BS radical and styrene. A bimolecular reaction rate coefficient of $k_{react} = (3.8 \pm 0.2) \times 10^8$ M^{-1} s^{-1} is deduced and 22 ± 1 % of the initially formed BS radicals are converted to the BS-St radical in neat styrene solution.

1. INTRODUCTION

Reactive intermediates control the pathways of bimolecular chemical reactions in solution, but their short lifetimes make them challenging to observe experimentally.[1] One convenient method to generate these intermediates for further study is by photodissociation of stable molecules, because photo-induced homolytic bond cleavage creates radical intermediates that can be detected by transient absorption spectroscopy. One of the best-studied systems is photolysis of cyanogen iodide (ICN); its photodissociation, and the subsequent bimolecular reaction dynamics of the CN fragment, have been extensively investigated both in gas and liquid phases.[2-5] Recently, we reported the use of broadband sub-picosecond transient electronic absorption spectroscopy (TEAS) and transient vibrational absorption spectroscopy (TVAS) to map out the production, solvation and reactive loss of CN radicals in several solvents.[6-10] In the current study, we focus on the reaction dynamics of a larger molecular system. We choose the reactions of aromatic thiyl radicals because of their significance in chemical synthesis.[11-13] Aromatic disulfide or thiol systems serve as precursors, and their photochemistry has been relatively well studied because aromatic thiyl radicals show clear and strong absorptions in the ultraviolet and visible (UV/vis) regions.[13]

Photodissociation of aromatic disulfide systems on sub-picosecond time scales was intensively explored in the late 1980s and 1990s.[14-18] Scott et al. investigated the simplest aromatic disulfide, diphenyl disulfide in the liquid phase and focused on geminate recombination dynamics of the resulting phenylthiyl radical by applying a diffusion model.[18] Lochschmidt et al. examined the photodissociation dynamics of bis(julolidine) disulfide in both polar and apolar solvents, and observed rapid formation of julolidylthiyl radicals within 130 fs and subsequent geminate recombination of the radicals, as well as production of a radical dimer.[17] More recent investigations have concentrated on the generation of aromatic thiyl radicals by

photolysis of the corresponding aromatic thiol compounds, using a combination of high level *ab initio* calculations and experiments.[19-22]

Reactions of thiyl radicals with alkenes or alkynes, known as thiol-ene reactions, have been studied for a long time,[23] but have recently attracted greater attention from synthetic chemists interested in the "Click Chemistry" propounded by Sharpless and coworkers.[11] The objective of Click Chemistry is to establish a methodology for synthesis of functional molecules by simple, highly selective orthogonal reactions under mild conditions. The thiol-ene reaction has been identified as an example of an ideal click reaction.[12] The mechanism of the thiol-ene reaction was scrutinized by Ito et al. in the 1980s and reference [24] provides a review of the extensive literature. Various reaction systems were investigated, covering a number of combinations of aromatic thiyl radicals, from the photolysis of the corresponding disulfides, in various solvents including alkenes or alkynes. The effects of molecular oxygen on the reaction dynamics were also examined. Measurements traced the kinetics of removal of the thiyl radicals on the microsecond time scale using a flash photolysis method. The initial addition step in the thiol-ene reaction was proposed to be reversible, and molecular oxygen in the reaction system reacted with the carbon-centered radical adduct, resulting in a thiylperoxyl radical. The formation of thiylperoxyl radicals was subsequently confirmed by Zhang et al.[25]

In these flash-photolysis studies, the reaction products were not observed directly, but instead kinetics were deduced from the decay of spectral bands assigned to aromatic thiyl radicals. As we demonstrated previously in the ICN photochemical system, reaction intermediates and products can be successfully observed by TVAS, and we apply this methodology here to selected thiol-ene reactions. The thiyl radical selected for reactive studies is benzothiazole-2-thiyl (denoted as BS), and is generated by photolysis of 2,2'-dithiobis(benzothiazole) (BSSB). We examine the reaction of BS radicals with styrene, from photolytic creation until addition-product formation by sub-picosecond TEAS and TVAS. This combination of transient

spectroscopy methods provides a detailed picture of the pathways for reaction by monitoring both production and loss of intermediate species.

The BS radical was chosen because of its fast bimolecular reaction rate coefficient (e.g., 2.5×10^8 M^{-1} s^{-1} for BS reaction with styrene in cyclohexane solution) deduced from the microsecond flash photolysis work of Ito et al.[26] We chose styrene as an alkene source because of a relatively large (and negative) enthalpy change of this reaction system, which suppresses the reverse reaction.[27] Figure 1 compares calculated intrinsic reactions coordinates (IRC) for this chosen and two other thiol-ene reactions. Theoretical calculations predict that an expected addition product from BS reaction with styrene has strong infrared absorption bands which do not overlap with styrene spectral features. This discrimination between reactants and intermediates enables us to trace the product dynamics with TVAS.

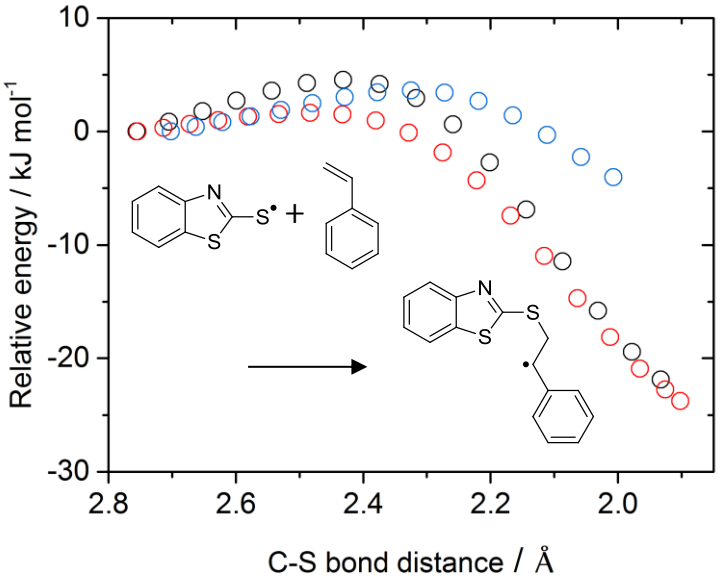

Figure 1: IRC calculation connecting separated BS and styrene to BS-St (red). For comparison, similar calculation results are shown for reaction of the simplest aromatic thiyl radical, phenylthiyl radical with styrene (black) and reaction of BS and a simple non-conjugated alkene, 2-methylpropene (blue).

2. EXPERIMENTAL DETAILS

2.1. Transient Absorption Spectroscopy

The transient absorption spectroscopy experiments were performed using an ultrafast laser system at the University of Bristol. The methods used for TEAS and TVAS measurements have been described previously,[28] therefore only a brief description relating directly to the current study is provided here.

Photochemistry of 2,2'-dithiobis(benzothiazole) (99%, Sigma Aldrich) was studied in solutions of toluene, methanol, cyclohexane, chloroform (all Analytical Grade, Sigma Aldrich), deuterated chloroform (99.8 atom % D, Sigma Aldrich) and styrene (≥ 99%, Sigma Aldrich). All solvents were used as received, with the exception of the styrene, which was passed through a basic aluminum oxide column before use to remove the inhibitor, 4-*tert*-butylcatechol. However, tests with the unpurified styrene showed no effect from the inhibitor over our experimental time range (up to 1.3 ns).

Measurements were carried out in a Harrick cell with CaF_2 windows separated by a PTFE spacer and sample solutions were circulated by a peristaltic pump. The UV excitation wavelength was 330 nm for both TEAS and TVAS experiments unless otherwise specified. This wavelength was chosen to avoid strong absorption by styrene; Figure 2 shows the steady state UV/visible absorption spectra of BSSB solutions, and compares to the absorption by styrene. All experiments were carried out with an air head-space in the sample reservoir, and without purging O_2 from the sample solutions, because no obvious influence from molecular oxygen on the spectral band shapes or reaction kinetics was seen under our experimental conditions.

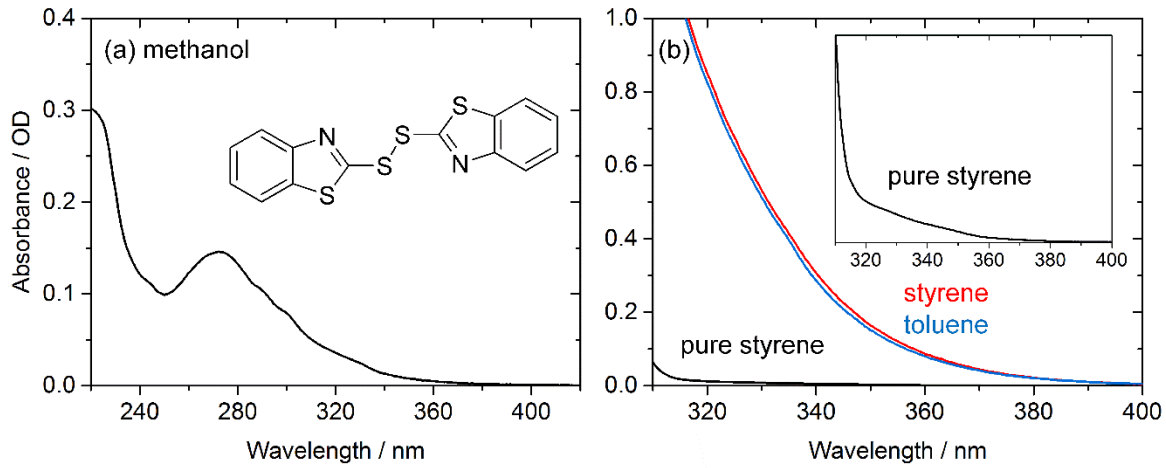

Figure 2: Steady state UV/vis absorption spectra. (a) 0.24 mM BSSB in methanol. (b) 5.5 mM BSSB in styrene (red) and toluene (blue). Inset: magnified view of the corresponding spectrum of pure styrene. Each spectrum was taken using a 380 μm pathlength sample.

2.1.1 Transient Electronic Absorption Spectroscopy

The thickness of the spacer in the Harrick cell used for TEAS measurements was 380 μm. Concentrations of the BSSB in styrene and toluene solutions were 5.5 mM, which was selected to give a sample absorbance of ~0.5 OD (for the 380 μm spacer) at the 330-nm excitation wavelength. The absorption ratio at 330 nm for styrene / BSSB is ~0.008 at this concentration (Figure 2). Due to the low solubility of BSSB in methanol, concentrations of methanol solutions were limited to 0.24 mM. A 300-nm pump wavelength was therefore used to increase signal intensities, and comparison of spectra with 300-nm and 330-nm pump wavelengths did not show obvious difference in spectral band shapes and kinetics. The pump laser energy was adjusted to 800 nJ / pulse for the methanol solution, and 200 nJ / pulse for the toluene and styrene solutions; the lower values were necessary for the latter two solutions because relatively large transient signals were observed from the solvents at the higher input power.

2.1.2. Transient Vibrational Absorption Spectroscopy

The TVAS measurements used a 100 μm thick spacer in the Harrick cell to minimize the effects of strong absorptions from the solvents. Concentrations of BSSB in styrene and toluene solutions were 7.2 mM, corresponding to almost the maximum solubility in both solvents, giving optical densities of 0.17 OD at 330 nm with the 100 μm spacer.

2.2. Computational Methods

Calculations of the optimized ground state geometries of BSSB, styrene and the addition-product radical (denoted as the BS-St radical), associated harmonic vibrational frequencies, IRCs, and electronic absorption spectra were performed using the Gaussian 09 package.[29] The B3LYP density functional,[30, 31] with the 6-311++G(3df,3pd) basis set, was chosen for all calculations because of a good balance between computational efficiency and reliability. Calculations of absorption spectra used time-dependent density functional theory (TDDFT) methods.

The potential energy curves (PECs) along the S-S bond distance of BSSB, and the vertical excitation energies and transition dipole moments of BS were calculated using the Molpro package.[32] For qualitative discussion, the PECs of the relatively large molecule, BSSB were calculated using the state averaged complete active space self-consistent field (SA-CASSCF) method with a 6-31G(d) basis set. The geometries at each S-S bond distance were optimized with the Gaussian 09 package at the B3LYP/6-311++G(3df,3pd) level of theory. Then, complete active space with second-order perturbation theory (CASPT2) energies were calculated using the SA-CASSCF result as a reference wavefunction. An imaginary level

shift of 0.4 a.u. was used for all of the CASPT2 calculations to avoid intruder state problems. These calculations included ten electrons in ten active orbitals (10/10) comprising the S-S σ bond, the corresponding S-S anti-bonding σ*, the four π and the four corresponding π* orbitals. Each π and π* orbital is comprised of symmetric π or π* orbitals on each benzothiazole ring. During the geometry optimizations for the PEC calculations, the dihedral and torsional angles between the two benzothiazole rings were frozen at the ground state equilibrium geometry values. The reason for the use of the fixed angles is that when full geometry optimizations were allowed, calculations at the longer S-S bond lengths showed sandwich like π-complexes between the two BS radicals. These types of complex are expected to form on time scales of a few ps by geminate recombination and are not considered important during the photodissociation of BSSB, which takes place with a time constant of ~200 fs, as discussed later.

For the calculation of the transition dipole moments of the BS radical, the ground state geometry was optimized using Møller-Plesset second-order perturbation theory (MP2) and the aug-cc-pVTZ basis set,[33, 34] and subsequently SA-CASSCF(9/9)/aug-cc-pVTZ calculations were carried out using the Molpro package. The (9/9) active space comprised the singly occupied sulfur $3p_x$, four π and the corresponding π* orbitals. The vertical transition energies were calculated at the CASPT2(9/9)/aug-cc-pVTZ level of theory using the SA-CASSCF result as a reference wavefunction.

3. RESULTS AND DISCUSSION

The photo-induced reaction dynamics of BSSB following UV excitation are unraveled by a combination of TEAS and TVAS. We discuss the results of TEAS measurements first because the formation, solvation and loss of the BS radical can be observed directly as a consequence of its relatively large molar extinction coefficient in the UV/vis region ($\varepsilon_{580\ nm}$ = 8500 $cm^{-1}\ M^{-1}$).[26] The interpretation of TEAS results is followed by presentation and analysis of TVAS data. In contrast to the TEAS measurements, in which the absorption bands are typically broad and therefore information about reaction products is often masked, the sharper IR bands seen in TVAS measurements characterize the products and distinguish them from the BS radical.

3.1. Transient Electronic Absorption Spectroscopy

TEAS studies of BSSB were performed in solution in methanol, toluene and styrene. The TEAS of the methanol solution was performed to obtain fundamental information on the photodissociation of BSSB because in toluene and styrene solutions, transient signals from the solvents themselves complicated the interpretation of the kinetics of the BS radical. The TEAS of BSSB in toluene was examined to compare with measurements in styrene because toluene has a similar chemical structure to styrene, but does not have an active double bond for thiol-ene reactions. Although our TEAS system covers the probe wavelength region from ~330 nm to 625 nm, for the measurements in the toluene and styrene solutions in which the 330-nm excitation pump wavelength was employed, any transient absorption signals located at wavelengths shorter than ~345 nm were masked by the pump laser light.

3.1.1. TEAS of BSSB in methanol solution

Figure 3 shows TEA spectra of BSSB in methanol. In Figure 3(a), two bands are evident at 345 and 584 nm. These two bands clearly show slower rises than the instrument response function of 150 fs deduced from pure methanol spectra (Figure S1 of the Electronic Supplementary Information), and grow at almost the same rate, as is shown in the inset to Figure 3(b). The time constant of ~200 fs for the growth of the band at 584 nm is deduced by a Gaussian convolution using the instrument response function time. A similar analysis of the time-dependence of the band at 345 nm was unsuccessful, most likely because of stronger background absorption in this region.

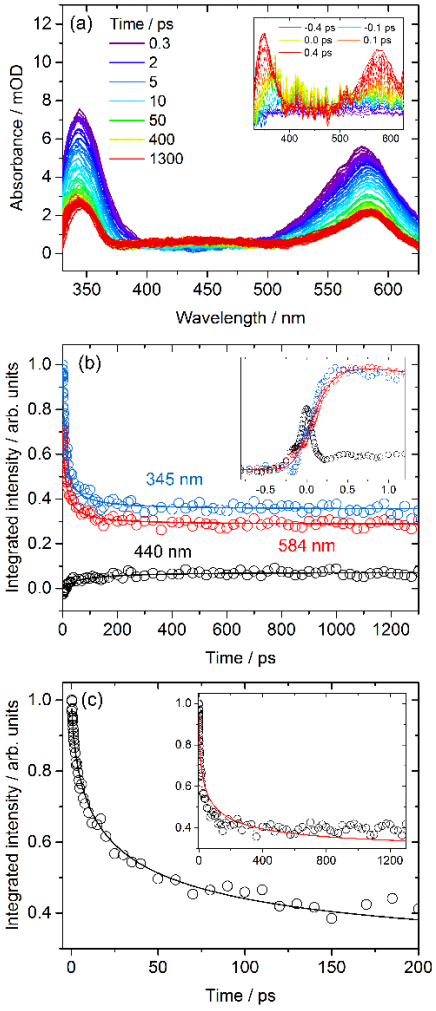

Figure 3: (a) Transient electronic absorption spectra of 0.24 mM BSSB in methanol following 300-nm excitation. Inset: spectra from the first 1 ps corrected for methanol features (see below). (b) Time-dependence of the BS radical and the BS radical dimer obtained at specific wavelengths; blue: 345 nm, red: 584 nm, black: 440 nm. The solid lines represent biexponential fitting of the band intensities. The integrated band intensity at 584 nm is multiplied by a factor of 0.8 for clarity. The inset shows integrated band intensities at 345 nm, 584 nm and 440 nm for the first 1.2 ps, and a fitting to a Gaussian convoluted rise and decay for the band at 584 nm (solid line). Methanol contributes a significant absorption while the pump and probe pulses overlap in time. The spectra and kinetic traces in the inset were therefore obtained by subtracting the spectra of pure methanol from the corresponding spectra of BSSB in methanol solution. The time zero was determined from TEA spectra of pure methanol (Figure S1). Time constants for the rise in signals (~200 fs) were deduced by Gaussian convolution using an instrument response function of 150 fs (Figure S1). (c) Fitting of the band intensity (0.3 – 200 ps) at 584 nm to the diffusion model of Eq. (1). The contact distance was fixed to R = 9.3 Å. Inset: the solid red line represents the best fitting result over the whole temporal range.

The band at 584 nm shifts to longer wavelengths with a time constants of ~2 ps. This peak shift can be understood as a result of solvation by methanol molecules. However, a peak shift is not observed for the band centred at 345 nm; this is because the band position is close to the edge of the probe light range, which conceals the shift. A strong absorption band lying at 450 - 600 nm depending on the chemical structure of the aromatic disulfide, is a characteristic feature of aromatic thiyl radicals.[13, 35, 36] In addition, the band position is the same as that of BS radicals observed by microsecond flash photolysis.[26] Therefore, the band at 584 nm is assigned to BS radical formed by photolysis of BSSB. This assignment is further supported by the calculated electronic absorption bands of the BS radical listed in Table 1 and the potential energy curves for BSSB shown in Figure 4. These computed PECs indicate that the first and third excited singlet states of BSSB are dissociative along the S-S coordinate. On the basis of CASSCF calculations, the S_1 state is mainly comprised of one electron excitations from the two π orbitals (HOMO or HOMO-1) to the σ^* orbital (LUMO). The precise photodissociation mechanism of BSSB is uncertain following 300 or 330-nm UV absorption. However, the PECs and steady state UV/vis spectra illustrated in Figure 2(a) suggest that the BS radical forms by either direct excitation to the dissociative S_1 state or absorption to the bound S_2 state followed by coupling onto the dissociative S_1 state at a conical intersection (CI1 in the figure). The S_1 state thereafter encounters a second conical intersection (CI2), resulting in ground state BS radicals. Table 1 also summarizes the computed excitation wavelengths and oscillator strengths for BSSB absorption bands. Direct excitation from the S_0 state to the S_1 state is weak, but the shoulder in the absorption band above 300 nm in Figure 2(a) might correspond to this $\pi\sigma^*$ transition.

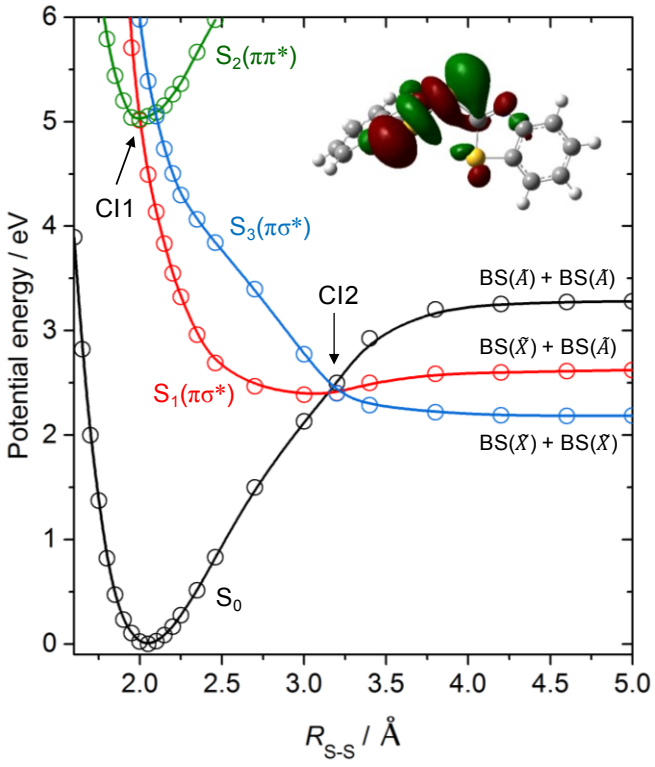

Figure 4: Potential energy curves along the S-S bond distance ($R_{S\text{-}S}$) for BSSB calculated at the CASPT2(10/10)/6-31G(d) level. The lowest bound excited singlet potential curve and the lowest two dissociative πσ* states are shown. The LUMO at the equilibrium geometry is also plotted.

Table 1: Calculated electronic absorption wavelengths and oscillator strengths for the indicated species using the TD-DFT/B3LYP/6-311++G(3df,3pd) method. For the BS and BS-St radical, only excitations with oscillator strengths ≥ 0.01 are shown.

BSSB		BS radical		BS-St radical	
Excitation wavelength / nm	Oscillator Strength	Excitation wavelength / nm	Oscillator Strength	Excitation wavelength / nm	Oscillator Strength
304 (πσ*, LUMO ← HOMO)	0.000	514	0.116	473	0.022
301 (πσ*, LUMO ← HOMO-1)	0.005	328	0.095	388	0.010
275 (ππ*)	0.178	302	0.121	357	0.013

Following the rapid growth of the band at 584 nm, it decays with time constants of $\tau_1 = 3.7 \pm 0.4$ ps and $\tau_2 = 50 \pm 4$ ps if biexponential fitting is employed. Similar time scales have been reported previously for the decay of aromatic thiyl radicals formed by photolysis of aromatic disulfides, and attributed to recombination to reform the parent aromatic disulfide.[14, 18] We therefore assign the decay to geminate recombination of the BS radicals to produce parent molecule BSSB. The results of fitting time-dependent integrated band intensities with bi-exponential functions are summarized in Table 2.

Table 2: Exponential time constants (τ_i), relative amplitudes (a_i) and long-time offsets from fits to time-dependent band intensities observed in TEAS measurements.

Solvent	Band position / nm	τ_1 / ps	a_1 / %	τ_2 / ps	a_2 / %	τ_3 / ps	a_3 / %	Offset / %
Methanol	345	4.2 ± 0.5	37 ± 2	54 ± 6	27 ± 2	-	-	36 ± 1
	440	6.2 ± 2.2	61 ± 10	67 ± 13	39 ± 9	-	-	-
	584	3.7 ± 0.4	35 ± 1	50 ± 4	29 ± 1	-	-	36 ± 1
Toluene	345	4.9 ± 0.6	36 ± 2	48 ± 7	22 ± 2	-	-	42 ± 1
	440	6.0 ± 2.1	64 ± 12	65 ± 13	36 ± 9	-	-	-
	588	3.2 ± 0.3	38 ± 2	50 ± 5	21 ± 1	8200 ± 900	41 ± 1	-
Styrene	345	2.3 ± 0.4	34 ± 3	23 ± 3	35 ± 2	388 ± 34	23 ± 1	8 ± 1
	360	-	-	-	-	314 ± 21	-	-
	445	-	-	-	-	323 ± 39	-	-
	590	1.6 ± 0.2	55 ± 6	27 ± 3	23 ± 1	305 ± 13	22 ± 1	-

Bultmann et al. analyzed cage recombination of *p*-aminothiophenoxy radicals generated photolytically from bis(*p*-aminophenyl)disulfide using a geminate recombination model.[14] According to the model, the survival probability $\Phi(t)$ is described by:

$$\Phi(t) = 1 - \frac{R}{r_0}\left\{\frac{k_{rev}}{k_{rev}+4\pi RDN_A}\right\}\left[\operatorname{erfc}\left\{\frac{r_0-R}{2\sqrt{Dt}}\right\} - \exp\{P^2Dt + P(r_0-R)\}\operatorname{erfc}\left\{P\sqrt{Dt}+\frac{r_0-R}{2\sqrt{Dt}}\right\}\right] \quad (1)$$

In this expression,

$$P = \frac{1}{R}\left\{\frac{k_{rev}+4\pi RDN_A}{4\pi RDN_A}\right\} \quad (2)$$

and erfc is the complementary error function. The model considers a nascent radical pair which is initially separated by a distance r_0, and undergoes reactive encounters at a contact (reactive) distance R, with a second-order rate coefficient k_{rev}. N_A denotes the Avogadro constant and D is a diffusion coefficient represented by the Stokes-Einstein equation:

$$\mathrm{D} = k_B T/6\pi\eta a \quad (3)$$

In Eq. (3), k_B denotes the Boltzmann constant, T the absolute temperature, η the viscosity of the solvent and a the hydrodynamic radius. We estimated the hydrodynamic radius a = 3.15 Å using the van der Waals volume of a BS radical, and by treating the molecule as a sphere. This model does not consider solvation, which stabilizes radicals and suppresses recombination, and therefore underestimates the survival probability at longer time delays (as seen in the inset to Figure 3(c)).[14] Hence, we only used the first 200 ps of the normalized integrated band intensity for our fitting.

During our data fitting, R was fixed to 9.3 Å, corresponding to twice the distance from the center of one benzothiazole ring to the center of the sulfur-sulfur bond of the parent BSSB. Distances were deduced from the equilibrium geometries obtained from our DFT calculations. The same method was used by Scott et al. to estimate the contact distance for photodissociation of diphenyl disulfide.[18] As Figure 3(c) illustrates, the observed time dependence of the band intensity is fit well with equation (1), and we deduce a geminate recombination rate coefficient of $k_{rev} = (3.7 \pm 0.2) \times 10^{10}$ M^{-1} s^{-1} and an initial separation distance $r_0 = 9.5 \pm 0.3$ Å. These k_{rev} and r_0 values are in reasonable agreement with previously reported values for the geminate recombination of *p*-aminothiophenoxy radicals.[14] We note that this k_{rev} also includes a contribution from competitive formation of a sandwich-type BS radical dimer, and we rewrite this rate coefficient as $k_{rev+dimer}$ later in this section.

The recombination is observed to be incomplete, because the integrated band intensity remains almost constant from approximately 200 ps until the limit of our experimental time delay (1.3 ns). The reported lifetimes of aromatic disulfides which have escaped from a solvent cage are in the microsecond range,[24, 26, 35, 36] therefore the observed almost flat integrated absorbance is quite reasonable. On the basis of the integrated band intensities and exponential fittings shown in Figure 3(b) and Table 2, (36 ± 1) % of the initially formed BS radicals survive at our longest time delay.

The band at 345 nm is also assigned to the BS radical because its fast rise and its decay kinetics, which are summarized in Table 2, are the same as for the band at 584 nm within the 2 SD uncertainties. Based on the vertical excitation energies (which are not corrected for solvent effects) and transition dipole moments reported in Table 3, the band at 345 nm can be ascribed to the overlapping $\tilde{C} \leftarrow \tilde{X}$ and $\tilde{D} \leftarrow \tilde{X}$ transitions of the BS radical, and the band at 584 nm is assigned to a mixture of the $\tilde{A} \leftarrow \tilde{X}$ and $\tilde{B} \leftarrow \tilde{X}$ transitions. Photodissociation studies in the gas phase, transient absorption spectroscopy in the liquid phase, and *ab initio*

calculations for the *p*-methylthiophenoxy radical generated from photolysis of *p*-methylthiophenol all suggest that absorption from the $\tilde{A}$ state may contribute to transient spectra of photochemically generated thiyl radicals.[19-22] Careful inspection of the inset in Figure 3(a) identifies an absorption feature located at around 400 - 480 nm at early time delays (~ 100 fs) that may be a candidate. However, this feature has its maximum absorbance at time zero and can be observed only while the pump and probe beams are overlapped in time (Figure 3(b) inset). This feature might be derived from incomplete subtraction of pure methanol spectra from the spectra of BSSB in methanol solution, but judging from the kinetic traces at 345 nm and 584 nm presented in the inset of Figure 3(b), it is likely that the pure solvent spectrum is almost completely subtracted. Therefore, we conclude that this feature is an absorption from an excited state, but one that is more likely to belong to the BSSB parent molecule than to an excited state of the BS radical. This difference, when compared to *p*-methylthiophenoxy, may be associated with the larger energy separation between the $\tilde{A}$ and $\tilde{X}$ states (2.39 eV) for the BS radical.[22]

Table 3: Calculated excitation energies and transition dipole moments for the BS radical, obtained at the CASPT2(9/9)/aug-cc-pVTZ and CASSCF(9/9)/aug-cc-pVTZ levels of theory.

Transition	Excitation energy / eV	Excitation wavelength / nm	Transition dipole moment / Debye
$\tilde{A} \leftarrow \tilde{X}$	2.39	520	2.30
$\tilde{B} \leftarrow \tilde{X}$	2.55	486	1.31
$\tilde{C} \leftarrow \tilde{X}$	3.92	316	0.94
$\tilde{D} \leftarrow \tilde{X}$	3.96	313	1.24
$\tilde{E} \leftarrow \tilde{X}$	4.45	279	1.86

Further inspection of Figure 3(a) indicates that there is a broad band centered at 440 nm which grows with time. This type of broad feature is observed in addition to the two prominent bands at 345 nm and 584 nm regardless of excitation wavelength or choice of solvent (Figure S2). As Figure S2 shows, the band intensity of the broad band is stronger in cyclohexane solution than other solvents. Similar bands for aromatic disulfides have been reported previously, with stronger band intensity in apolar solvents, and assigned to a sandwich type π-stacked radical dimer. We therefore assign this broad feature to the BS radical dimer adopting this stacked structure.[15, 17] The time constants for the formation of BS radical dimer (see Table 2) are deduced to be $\tau_1 = 6.2 \pm 2.2$ ps and $\tau_2 = 61 \pm 10$ ps by fitting to integrated absorbances for this band, obtained at various time delays by spectral decomposition with the KOALA program.[37] Figure S3 shows an example of this spectral decomposition. The agreement between the time constants for recombination of the BS radical and growth of the BS radical dimer band supports this assignment.

The deduced rate coefficients k_{rev} should therefore be re-interpreted because the following two competing processes result from recombination of two BS radicals:

$$\mathrm{BSSB} \underset{k_{rev}}{\overset{h\nu}{\rightleftharpoons}} 2\,\mathrm{BS} \xrightarrow[k_{dimer}]{} (\mathrm{BS})_2 \qquad (4)$$

Here, $(BS)_2$ represents the BS π-stacked dimer. The rate coefficients k_{rev} and k_{dimer} together control the rate of loss of BS and growth of $(BS)_2$, and we therefore replace them by $k_{rev+dimer} = (3.7 \pm 0.2) \times 10^{10}$ M^{-1} s^{-1}, where $k_{rev+dimer} = k_{rev} + k_{dimer}$.

3.1.2. TEAS of BSSB in toluene solution

Figure 5(a) and (b) illustrate TEA spectra of BSSB in toluene, integrated band intensities and kinetic fits. In toluene solution, the shapes of spectra, peak positions and the kinetics are

similar to the methanol solution, except for the larger time-dependent red-shift of the band at 588 nm and some characteristics of the kinetic trace at 588 nm. The integrated intensities for the band at 345 nm indicate that (42 ± 1) % of the initially formed BS radicals survive at the longest time delay under our experimental conditions. In contrast to the kinetic trace of the band centred at 345 nm, for which the integrated band intensity is almost constant after ~200 ps, the band at 588 nm shows a small but continuous decrease in absorbance until the longest time delay. A time constant of $\tau_3 = 8.2 \pm 0.9$ ns is obtained by fitting this decay with a single exponential function. Transient absorption by toluene is the cause of the apparent differences in the time dependence of these two bands. Although toluene does not apparently absorb 330-nm pump light, the pure toluene shows transient spectra in response to laser pulses at this wavelength (Figure S4). The shapes of the spectra resemble prior reports and the features are therefore assigned to two-photon excitation of toluene.[38] The contribution from the toluene to our transient spectra could be mostly, but not completely, removed by decreasing the pump power from 800 nJ/pulse to 200 nJ/pulse. However, the longer time decay in the intensity of the 588 nm feature in BSSB / toluene solutions could be almost entirely eliminated by subtracting the spectra of pure toluene from the corresponding BSSB in toluene spectra.

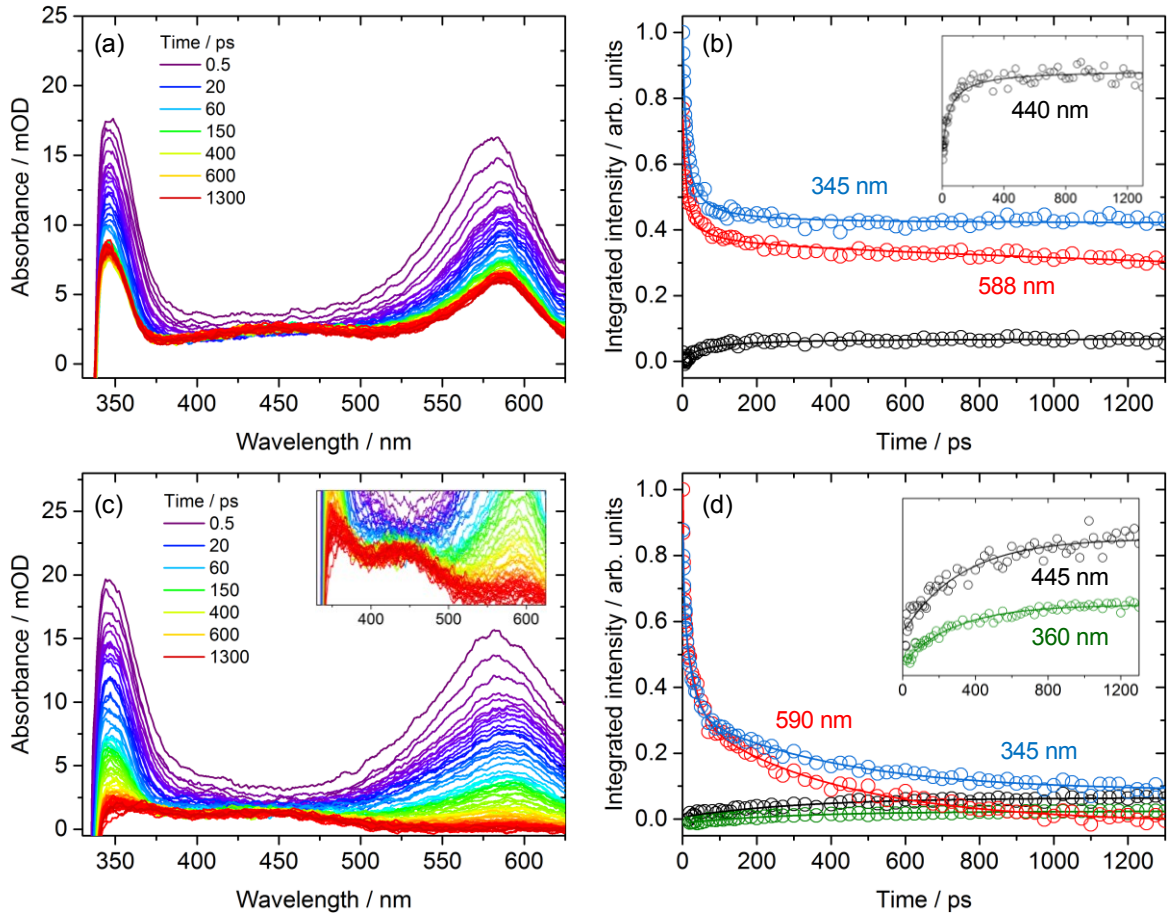

Figure 5: (a) Transient electronic absorption spectra of 5.5 mM BSSB in toluene solution following 330-nm excitation at a pump energy of 200 nJ/pulse. (b) Time-dependence of the BS radical and the BS radical dimer; blue: 345 nm, red: 588 nm, black: 440 nm. The inset shows an expanded view at 440 nm. (c) Transient electronic absorption spectra of 5.5 mM BSSB in styrene solution following 330-nm excitation at a pump energy of 200 nJ/pulse. The inset shows an expanded view of the product bands. (d) Time-dependence of the BS radical and the BS-St radical; blue: 345 nm, red: 590 nm, green: 360 nm, black: 445 nm. The inset shows an expanded view of the 360-nm and 445-nm data. The solid lines in (b) and (d) represent exponential fittings of the band intensities.

3.1.3. TEAS of BSSB in styrene solution

In styrene solution, the shapes of spectra at early time delays resemble those observed for solutions of BSSB in toluene, as shown in Figure 5(c). However, the kinetics deduced from

the BS radical bands at 345 nm and 590 nm are dramatically different from those seen in toluene; for example, the latter band completely disappears within the limit of our experimental delay time (Figure 5(d)). This additional decay component corresponds to a reaction of the BS radical with styrene molecule, as is discussed later. The faster geminate recombination to BSSB and the BS radical dimer will mostly occur within the initial solvent cage whereas the slower reaction with solvent molecules most probably takes place after BS radicals have escaped this solvent cage. Accordingly, the following reaction scheme (5), with radical recombination treated by the method discussed above, can in principle be employed to extract kinetic information:

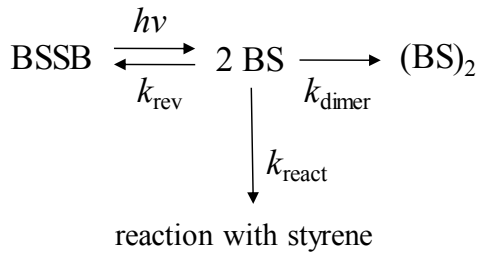

(5)

Styrene is present in considerable excess over BS radicals, and we therefore define a pseudo first-order rate coefficient for the bimolecular reaction $k'_{\mathrm{react}} = k_{react}[\mathrm{styrene}]$.

This more complicated kinetic scheme prevents a full analysis of the geminate and diffusive recombination in competition with reactive removal of BS radicals, so we instead employ a phenomenological tri-exponential fitting. Table 2 reports the outcomes. The shortest two time constants, τ_1 and τ_2 are attributed to radical recombination steps, and τ_3 characterizes the reactive loss of BS with styrene. As was the case with toluene solution, styrene itself also shows a prompt transient signal (Figure S5), and therefore the fitting of early kinetics to equation (1) is unreliable. The signal from pure styrene can be effectively reduced by decreasing the pump power (e.g. comparison between Figure 5(c) and Figure S5(c)), but it is still weakly observed even at the low pump pulse energy of 200 nJ/pulse. The transient signal

from pure styrene decays with a time constant of 23 ps and almost completely disappears after ~200 ps; therefore, this signal has practically no influence on the value of k'_{react} (= $1/\tau_3$) and causes a difference only in the deduced values of τ_1 and τ_2. Accordingly, we derive a pseudo-first order rate coefficient k'_{react} = (3.3 ± 0.2) × 10^{-3} ps^{-1}, and 22 ± 1 % conversion of the BS radical to the reaction product.

The integrated intensity for the band at 345 nm also shows an obvious additional decay component, but the kinetics are different from the band at 590 nm. This discrepancy is a consequence of a product band lying under the BS radical absorption band, as discussed below. Spectral decomposition with the KOALA program suggests that there are broad bands lying underneath the absorption from the BS radical over the range from ~345 nm to 500 nm (Figure 5(d)). Similar features were observed in the toluene and methanol solutions, but the kinetics differ in styrene solution. In particular, the bands show continuous growth over our experimental time range. Our analysis assumes that there are two growing bands centered at 360 nm and 445 nm (see Figure S6 for an example of spectral decomposition), and fitting of their integrated band intensities to single exponential functions gives time constants of τ_3 = 314 ± 21 ps for the band at 360 nm and τ_3 = 323 ± 39 ps for the band at 445 nm. To deduce the above rate coefficients, we used the integrated band intensities from 20 ps to 1300 ps and neglected the first 20 ps. In this early time window, a faster rising component is apparent for the band centered at 445 nm, which is possibly the formation of BS radical dimer.

Both of the extracted time constants for the band at 360 nm and 445 nm are consistent with the decay component τ_3 for the band at 590 nm (τ_3 = 305 ± 13 ps). Considering the above agreement in rate coefficients, the experimental result that the two continuously growing bands are not observed in other solution systems, and assuming that these two bands derive from the same species, the 360-nm and 445-nm features are assigned to an addition product of BS radical to styrene formed through the following reaction scheme:

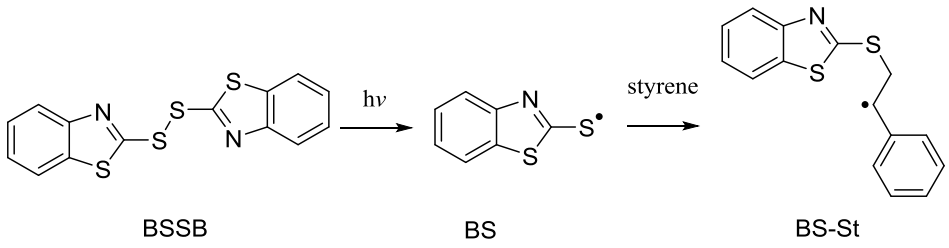

(6)

This assignment is further supported by the TD-DFT calculations for the BS-St radical presented in Table 1. A more detailed discussion is provided in Section 3.2.2 in conjunction with analysis of TVAS experiments.

3.2. Transient Vibrational Absorption Spectroscopy

TVAS experiments were performed for BSSB over the probe wavenumber range of 1220 cm^{-1} - 1440 cm^{-1} in both toluene and styrene solutions following UV excitation. In preliminary survey experiments, TVAS measurements were also made in the 1440 - 1600 cm^{-1} region, but no obvious signals were obtained except for a bleach feature of the BSSB at 1465 cm^{-1} (not shown).

3.2.1. TVAS of BSSB in toluene and deuterated chloroform solutions

Figure 6(a) and (b) show TVA spectra of 7.2 mM BSSB in toluene following 330-nm excitation. Three negative-going bleach bands at 1236, 1310 and 1427 cm^{-1} are ascribed to reduction in the ground-state BSSB concentration induced by the pump light, and the assignment is confirmed by comparison with steady state FTIR spectra (Figure S7). In TVAS experiments, no absorption from pure toluene is observed in this spectral region when the 330-nm pump light is applied.

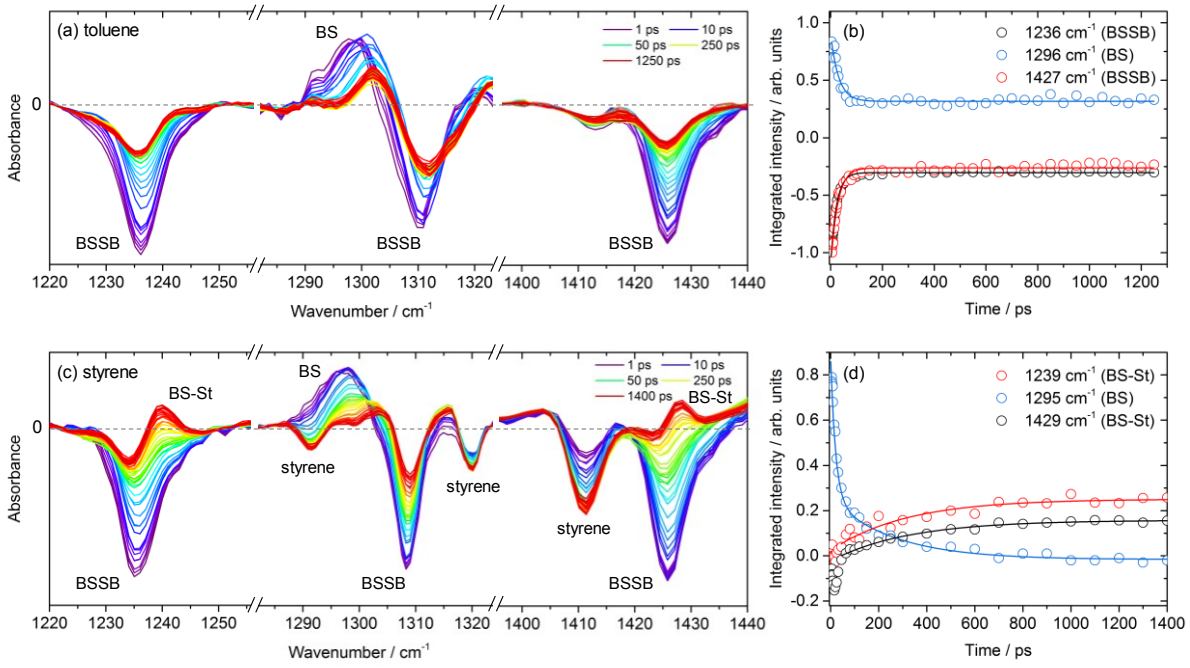

Figure 6: Transient vibrational absorption spectra of BSSB solutions following 330-nm excitation at a pump energy of 800 nJ/pulse. (a) 7.2 mM BSSB in toluene, and (b) time-dependence of band intensities. (c) 7.2 mM BSSB in styrene, and (d) time-dependence of band intensities. The solid lines in (b) and (d) represent exponential fittings of the integrated band intensities. Fits to the bands at 1239 and 1429 cm^{-1} omit the first 45 ps.

The outcomes of exponential fits to the intensities of TVAS bands are summarized in Table 4. The bleach bands at 1236 and 1427 cm^{-1} recover with time constants of 25 ± 1 ps for the former and 27 ± 2 ps for the latter if single exponential fitting is employed. In contrast to the TEAS measurements, fitting the integrated TVAS band intensities with single exponential functions sufficiently describes the observed early time kinetic traces. Comparison with the TEAS measurements suggests the bleach-recovery corresponds to geminate recombination of BS radicals to the parent BSSB, but we have to consider possible first-order decay processes such as: (i) fluorescence from a singlet excited state of BSSB; (ii) intersystem crossing of BSSB to

a triplet state; and (iii) non-radiative recovery of ground-state BSSB by internal conversion. Microsecond flash photolysis studies of the photodissociation of BSSB reported similarities in spectral features under both aerated and degassed solvent conditions,[26] which argues against ISC of BSSB to a triplet state. Aromatic disulfides show low fluorescence quantum yields (e.g., less than 10^{-4} for *p*-aminophenyldisulfide),[39] and we therefore discount fluorescence from an excited state of BSSB. On the other hand, quantum yields for photodissociation of aromatic disulfides are less than unity ($\Phi_{dissociation}$ = 0.048 – 0.57 depending on excitation wavelength),[40] and hence non-radiative process such as internal conversion back to the ground state of BSSB, perhaps through the conical intersection (CI2) shown in Figure 4, are likely to contribute to the bleach recoveries, in addition to geminate recombination.

Table 4: Exponential time constants (τ_i), relative amplitudes (a_i) and long-time offsets from fits to time-dependent band intensities observed in TVAS measurements.

Solvent	Band position / cm^{-1}	Attribution	τ_1 / ps	a_1 / %	τ_2 / ps	a_1 / %	Offset / %
Toluene	1236	BSSB	25 ± 1	73 ± 1	-	-	27 ± 1
	1301	BS	29 ± 3	65 ± 3	-	-	35 ± 1
	1427	BSSB	27 ± 2	76 ± 2	-	-	24 ± 1
Styrene	1239	BS-St	-	-	312 ± 68	-	-
	1295	BS	23 ± 2	71 ± 3	294 ± 32	29 ± 3	-
	1429	BS-St	-	-	325 ± 33	-	-

The integrated band intensities for the two bleach features at 1236 and 1427 cm^{-1} remain almost constant after ~200 ps, and approximately 25% of the initially formed bleaches remain at the longest time delay. The bleach recovery kinetics for the band at 1310 cm^{-1} differ because of spectral overlap with a positive band centered at lower wavenumber. This positive band

reaches its maximum absorbance within the effective time resolution of ~1 ps, and shows a peak shift from 1296 cm^{-1} at the earliest time delay to 1301 cm^{-1} with a time constant of ~12 ps. TVAS experiments of BSSB in deuterated chloroform with various pump wavelengths indicate that the degree of peak shift increases when using shorter wavelength pump light (Figure S8), suggesting the peak shift corresponds to vibrational relaxation of a photochemically produced species. The time constant for the decay of the band at 1296-1301 cm^{-1} is $\tau_1 = 29 \pm 3$ ps obtained by fitting to a single exponential function, and 35 ± 1 % of initial band intensity remains at the longest time delay. Judging from the time scale for the decay and the residual band intensity at later times, we assign the band at 1301 cm^{-1} to the BS radical. This assignment is further supported by the calculated infrared frequencies shown in Table 5.

In deuterated chloroform solution (Figure S8), a positive band at 1319 – 1322 cm^{-1} can be seen in addition to a band at 1302 cm^{-1}. This additional feature reaches its maximum absorbance within 1 ps and shows a peak shift to higher wavenumber with time. This band is therefore also assigned to the BS radical, with support from the computed infrared band wavenumbers reported in Table 5. However, the presence of the BSSB bleach band at 1310 cm^{-1} prevents us from determining if this band is resolved from the band at 1302 cm^{-1}. Since the corresponding band in the styrene solution is completely masked by a solvent bleach band, we do not discuss it further.

Table 5: Calculated fundamental infrared transition frequencies and intensities, and observed infrared frequencies for BS and BS-St radicals. Calculations used the Gaussian 09 package and the B3LYP functional with the 6-311++G(3df,3pd) basis set.

	Calculation		Experiment
	Frequency[a] / cm^{-1}	Intensity[b] / km mol^{-1}	Frequency / cm^{-1}
BS radical	1301	17	1301
	1316	21	1322 [c]
BS-St radical	1238	33	1239
	1310	8	1303
	1421	119	1429

[a] Calculated infrared frequencies over our experimental probe region (1220 cm^{-1} - 1440 cm^{-1}). The infrared positions presented in the table are corrected by a linear function obtained by comparing the experimental and calculated frequencies for BSSB (Figure S9).

[b] Only calculated bands with band intensities greater than 5 km mol^{-1} are shown.

[c] Confirmed in deuterated chloroform solution (Figure S8).

3.2.2. TVAS of BSSB in styrene solution

Figure 6(c) and (d) show TVA spectra of 7.2 mM BSSB in styrene following 330-nm excitation, together with integrated band intensities and kinetic fits. The spectra exhibit three bleach features attributed to the BSSB which are observed at the same positions as for the toluene solution measurements. A transient absorption band, initially centered at 1295 cm^{-1}, is assigned to the BS radical. The peak of this band shifts to higher wavenumber with time, just as was seen in toluene. Due to the spectral overlap, another band which is also assigned to the BS radical and seen in deuterated chloroform solution could not be confirmed in the styrene solution. Fitting the integrated band intensities at 1295 cm^{-1} to equation (4) gives $k'_{react} = 1/\tau_2 = (3.4 \pm 0.4) \times 10^{-3}$ ps^{-1}, and the rate coefficient is in reasonable agreement with the decay kinetics of the BS radical obtained by TEAS. In addition to these various bands, there are

also three negative bands at 1292, 1319 and 1413 cm^{-1} attributed to styrene on the basis of comparison with its steady state FT-IR spectrum (shown in Figure S7).

Furthermore, two bands at 1239 and 1429 cm^{-1} grow with time, and are clearly evident despite overlapping the bleach features at 1237 and 1427 cm^{-1}. Spectral decomposition with the KOALA program (see, for example, Figure S10) indicates that these two bands grow with time constants of 312 ± 68 ps for the band at 1239 cm^{-1} and 325 ± 33 ps for the band at 1429 cm^{-1}. These two features are not seen for BSSB in toluene (Figure 6(a)) or in pure styrene (Figure S11). Given that the time constants for these two bands match the second component of the decay of the BS radical in styrene solution obtained by TEAS and TVAS, they are assigned to the product of the BS radical addition reaction with styrene. This product is proposed to be the anti-Markovnikov type addition product, BS-St radical formed through reaction scheme (6). This assignment to the BS-St radical is also supported by the computed vibrational wavenumbers provided in Table 5: the calculated frequencies for the BS-St radical agree well with the observed positions. Based on the calculation in Table 5, the BS-St radical is also expected to show an absorption at around 1310 cm^{-1}. Careful inspection of the spectra in Figure 6(c) suggests a band at 1303 cm^{-1}, but the small intensity and spectral overlaps prevent analysis of its kinetics. Infrared band positions and intensities predicted by DFT calculations for the Markovnikov type addition product **1** are almost the same as for the anti-Markovnikov BS-St radical and we therefore could not distinguish these two BS-St radical products by TVAS. However, addition of a thiyl radical to an alkene or alkyne is known to favour the anti-Markovnikov pathway.[13, 41] Therefore, we followed this expected propensity in considering the adduct structure.

Two alternative candidates are also considered for reaction products responsible for the TVAS bands: the molecular oxygen adduct **2** (or **2'**) and the two-BS radical adduct **3**.

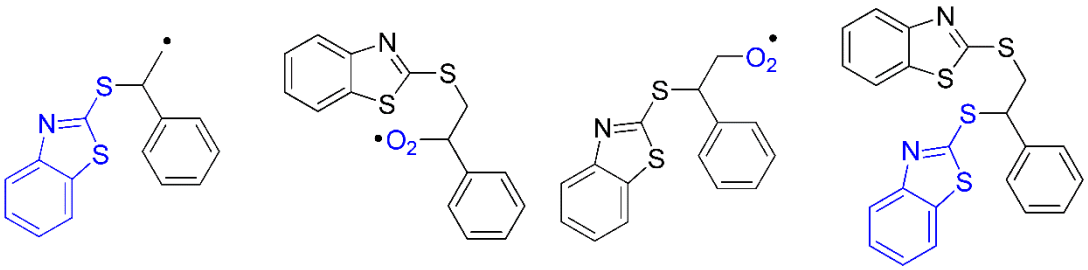

1 2 2’ 3

Ito *et al*. assumed that the BS-St radical reacts with molecular oxygen at a rate approaching the diffusion controlled limit,[26] by analogy with reactions of carbon-centered radicals with molecular oxygen.[42] However, as described in section 2.1, no obvious effects of molecular oxygen were observed over our shorter experimental time range. This is quite reasonable considering the equilibrium concentration of molecular oxygen dissolved in styrene solution exposed to air (1.4 mM at 25 ºC):[43] even if the reaction proceeded at a diffusion controlled rate, a bimolecular reaction between the BS radical and molecular oxygen is unlikely within our 1.3 ns upper limit. For these reasons, the first candidate **2** (or **2’**) and other such peroxy radicals are ruled out as contributors to the TVA spectra. We can also dismiss the second candidate **3** because the TEAS measurements in styrene showed growth of broad band(s) at 345 - 500 nm (Figure 5(c) and (d)) which we assigned to reaction products. Compound **3** is not expected to show any absorption bands in that spectral region.

In addition to the above arguments for band assignments, we also consider an alternative reaction pathway, in which a BS radical reacts with photoexcited styrene (denoted as [styrene]*) to make BS-St products:

$$\text{BSSB} \xrightarrow{h\nu} \text{BS} \xrightarrow[h\nu]{\text{styrene}} [\text{styrene}]^* \longrightarrow \text{BS-St} \qquad (7)$$

This consideration is necessary because styrene weakly absorbs the 330-nm pump light, as shown in Figure 2(b).

To explore this possibility, TVAS measurements were repeated for BSSB in styrene, but using 300-nm and 320-nm pump laser wavelengths. The outcomes are compared with the 330-nm excitation data in Figure 7. The ratio of maximum intensities of the BS-St radical absorption and the BSSB bleach ($\Phi_{rel} = I_{BS\text{-}St} / I_{BSSB}$) corresponds to a relative reaction quantum yield. With both the 330-nm and 320-nm pump light, this ratio is close to 0.25, but with 300-nm excitation, for which absorption by styrene is almost saturated under our experimental conditions (see Figure 2(b)), the ratio clearly decreases ($\Phi_{rel} = \sim 0.1$). If the BS-St radical forms through reaction scheme (7), the ratio $I_{BS\text{-}St} / I_{BSSB}$ at the 300 nm pump light should instead be larger than for 320-nm and 330-nm excitation. Accordingly, this possibility is ruled out.

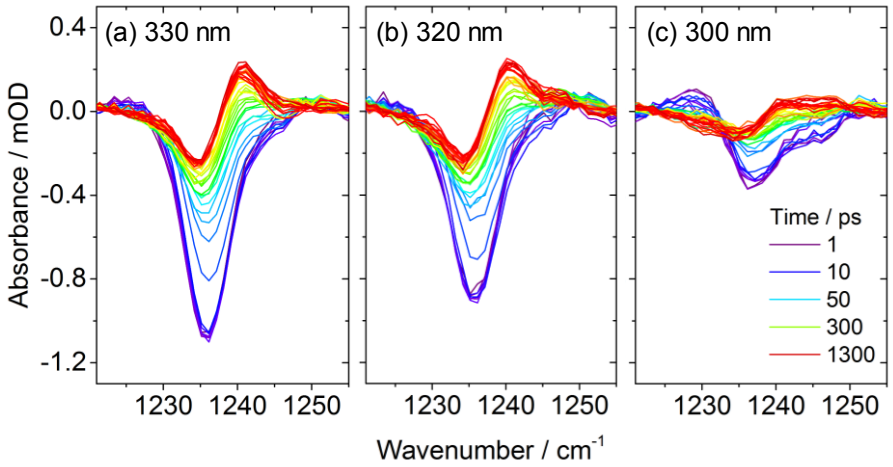

Figure 7: Transient vibrational absorption spectra of 7.2 mM BSSB in styrene following: (a) 330-nm; (b) 320-nm; and (c) 300-nm excitation.

3.3. Effect of Styrene Concentration on Bimolecular Reaction Rates

To obtain an accurate bimolecular reaction rate coefficient for the reaction of the BS radical and styrene, concentration dependence experiments were carried out both with TEAS and TVAS in styrene/toluene solutions. The BS-St radical band at 1239 cm^{-1} was used in preference to the band at 1429 cm^{-1} in TVAS experiments, because it is freer from interfering solvent absorptions. The TVAS measurements were restricted to ≥1.3 M styrene concentrations because of the small intensities of the product bands, especially at earlier time delays.

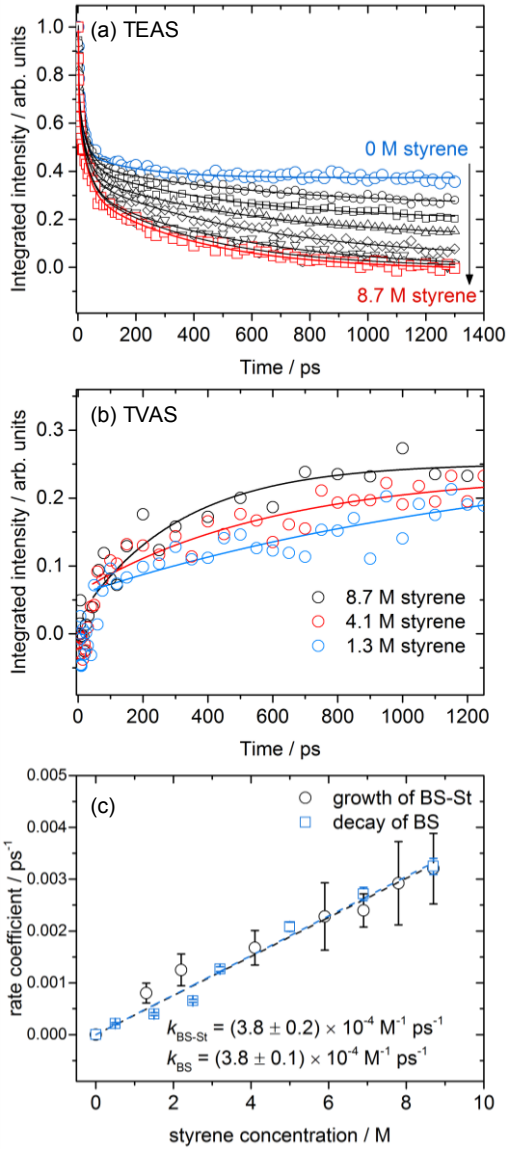

Figure 8: (a) Integrated intensities for the band at 590 nm obtained by transient electronic absorption spectra of 5.5 mM BSSB following 330-nm excitation at a pump energy of 200 nJ/pulse; in these measurements the styrene concentration was changed from 0 M (neat toluene) to 8.7 M (neat styrene). The solid lines represent tri-exponential fittings of the band intensities. (b) Integrated band intensities for the band at 1239 cm^{-1} obtained by transient vibrational absorption spectra of 7.2 mM BSSB at a pump power of 800 nJ / pulse. The styrene concentration was changed from 1.3 M to 8.7 M. The kinetics for three different styrene concentrations are shown in the figure as examples: blue: 1.3 M, red: 4.1 M, black: 8.7 M styrene solution. The solid lines are fits to single exponential functions that omit the first 45 ps. (c) Pseudo first order rate coefficients for the BS radical decay and the BS-St radical formation as a function of styrene concentration. The rate coefficients are obtained as reciprocals of exponential time constants for the decay of BS radical (by TEAS) and the growth of BS-St radical (by TVAS).

Figure 8(a) demonstrates that the slowest decay components in the 590-nm band in TEAS measurements, which are assigned to the BS radical, become faster with increasing styrene concentration. The growth of the TVAS band at 1239 cm^{-1}, assigned to the BS-St radical, is also accelerated by increasing styrene concentration (Figure 8(b)). Since the styrene is in considerable excess over the BS radical, pseudo first-order kinetic analysis is appropriate after the fast radical recombination processes. We therefore fitted the TEAS data to a tri-exponential function, and analysed the dependence of the τ_3 time constants on styrene concentrations. For TVAS data, single exponential fitting was adequate for time delays greater than 45 ps. In solutions containing toluene, the pseudo first-order reaction rate coefficients, obtained as $k'_{react} = 1/\tau_3$ contain an aforementioned contribution from the transient absorption feature observed from this solvent (see Section 3.1.2). The pseudo first-order rate coefficients were therefore corrected by subtracting a value $k_{\text{toluene}} = (1.2 \pm 0.2) \times 10^{-4}$ ps^{-1} before further analysis.

Figure 8(c) illustrates the linear dependence on styrene concentration of the pseudo first-order rate coefficients k'_{react} deduced from both TEAS and TVAS experiments. Linear fits of the data in Figure 8(c) give $k_{\text{BS-St}} = (3.8 \pm 0.2) \times 10^{-4}$ M^{-1} ps^{-1} from the growth of BS-St radicals (TVAS) and $k_{\text{BS}} = (3.8 \pm 0.1) \times 10^{-4}$ M^{-1} ps^{-1} from the decay of BS radicals (TEAS). Therefore, a bimolecular reaction rate coefficient of $k_{\text{react}} = (3.8 \pm 0.2) \times 10^{8}$ M^{-1} s^{-1} is deduced by taking an average of k_{BS} and $k_{\text{BS-St}}$. This bimolecular reaction rate coefficient is in reasonable agreement with the reported value of (2.5×10^{8} $M^{-1}s^{-1}$) for a similar reaction system (BSSB in styrene / cyclohexane solution) deduced by microsecond flash photolysis.[26]

4. CONCLUSIONS

The photochemical reactions of BSSB have been investigated by a combination of picosecond transient electronic absorption spectroscopy and vibrational absorption spectroscopy. The initial step of a thiol-ene reaction has been directly observed by detection of the addition reaction product: TVAS reveals the BS-St radicals formed by the addition of BS radicals to styrene.

The ground state BS radical is formed with a time constant of ~200 fs and shows two prominent electronic absorption bands at around 345 nm and 584 nm in methanol solution. The center wavelengths of these two bands shift slightly with change of solvents to cyclohexane, chloroform, toluene and styrene. The nascent BS radical decays with a rate coefficient of $k_{rev+dimer} = (3.7 \pm 0.2) \times 10^{10}$ M^{-1} s^{-1} in methanol solution, because of geminate recombination to the parent molecule BSSB and a BS radical dimer. Some of the BS radicals avoid these recombination pathways and persist over our full experimental time scale (~1.3 ns).

When BS radicals are generated photolytically from BSSB in styrene solution, a decay of the BS radical absorption bands is observed that is absent in methanol solution and for the reference studies in toluene. The time constant for this decay is 305 ± 13 ps, and corresponds to BS radical reaction with styrene. This reactive loss is confirmed by TVAS using a band assigned to BS radicals at 1295 cm^{-1}. Two product bands at 1239 cm^{-1} and 1429 cm^{-1} grow with respective time constants of 312 ± 68 ps and 325 ± 33 ps. These two bands are assigned to the BS-St radical formed through the addition reaction of a BS radical and styrene. When BSSB is photolysed in neat styrene, 22 ± 1 % of the initially formed BS radicals are converted to BS-St radicals. Analysis of both the loss of BS radicals and growth of BS-St products gives a bimolecular reaction rate coefficient, $k_{react} = (3.8 \pm 0.2) \times 10^{8}$ M^{-1} s^{-1} for the reaction of BS radicals with styrene in solution in toluene. The combination of TEAS and TVAS with

picosecond time resolution provides a comprehensive and quantitative picture of the early time process that occur in an example of this important class of thiol-ene reactions.

ACKNOWLEDGMENTS

We thank the European Research Council (ERC, Advanced Grant 290966 CAPRI) for financial support.

ELECTRONIC SUPPLEMENTARY INFORMATION AVAILABLE

All experimental data are archived in the University of Bristol's Research Data Storage Facility (DOI 10.5523/bris.16cgjutj3ipep1ela42jywkci9). The Supplementary Information contains TEA spectra of pure solvents used in this study (methanol, toluene and styrene), BSSB in cyclohexane (300 nm excitation), chloroform (240, 267, 300 and 330 nm excitation), examples of spectral decompositions, TVA spectra of pure styrene, BSSB in deuterated chloroform, steady state FT-IR spectra of BSSB in styrene, pure styrene, pure toluene and calculated infrared frequencies for BSSB

REFERENCES

1. B. K. Carpenter, J. N. Harvey and A. J. Orr-Ewing, *J. Am. Chem. Soc.*, in press 2016. DOI: 10.1021/jacs.6b01761
2. A. J. Orr-Ewing, *Annu. Rev. Phys. Chem.*, 2015, **66**, 119-141.

3. A. C. Crowther, S. L. Carrier, T. J. Preston and F. F. Crim, *J. Phys. Chem. A*, 2008, **112**, 12081-12089.
4. A. C. Crowther, S. L. Carrier, T. J. Preston and F. F. Crim, *J. Phys. Chem. A*, 2009, **113**, 3758-3764.
5. C. A. Rivera, N. Winter, R. V. Harper, I. Benjamin and S. E. Bradforth, *Phys. Chem. Chem. Phys.*, 2011, **13**, 8269-8283.
6. P. C. Coulter, M. P. Grubb, D. Koyama and A. J. Orr-Ewing, *J. Phys. Chem. A*, 2015, **119**, 12911-12923.
7. G. T. Dunning, T. J. Preston, S. J. Greaves, G. M. Greetham, I. P. Clark and A. J. Orr-Ewing, *J. Phys. Chem. A*, 2015, **119**, 12090-12101.
8. S. J. Greaves, R. A. Rose, T. A. A. Oliver, D. R. Glowacki, M. N. R. Ashfold, J. N. Harvey, I. P. Clark, G. M. Greetham, A. W. Parker, M. Towrie and A. J. Orr-Ewing, *Science*, 2011, **331**, 1423-1426.
9. D. Koyama, P. Coulter, M. P. Grubb and A. J. Orr-Ewing, *J. Phys. Chem. A*, 2015, **119**, 12924-12934.
10. R. A. Rose, S. J. Greaves, F. Abou-Chahine, D. R. Glowacki, T. A. A. Oliver, M. N. R. Ashfold, I. P. Clark, G. M. Greetham, M. Towrie and A. J. Orr-Ewing, *Phys. Chem. Chem. Phys.*, 2012, **14**, 10424-10437.
11. H. C. Kolb, M. G. Finn and K. B. Sharpless, *Angew. Chem. Int. Ed.*, 2001, **40**, 2004-2021.
12. C. E. Hoyle and C. N. Bowman, *Angew. Chem. Int. Ed.*, 2010, **49**, 1540-1573.
13. F. Dénès, M. Pichowicz, G. Povie and P. Renaud, *Chem. Rev.*, 2014, **114**, 2587-2693.
14. T. Bultmann and N. P. Ernsting, *J. Phys. Chem.*, 1996, **100**, 19417-19424.
15. Y. Hirata, Y. Niga, S. Makita and T. Okada, *J. Phys. Chem. A*, 1997, **101**, 561-565.
16. Y. Hirata, Y. Niga, M. Ohta, M. Takizawa and T. Okada, *Res. Chem. Intermed.*, 1995, **21**, 823-836.
17. A. Lochschmidt, N. Eilers-Konig, N. Heineking and N. P. Ernsting, *J. Phys. Chem. A*, 1999, **114**, 2587-2693.
18. T. W. Scott and S. N. Liu, *J. Phys. Chem.*, 1989, **93**, 1393-1396.
19. T. A. A. Oliver, G. A. King, D. P. Tew, R. N. Dixon and M. N. R. Ashfold, *J. Phys. Chem. A*, 2012, **116**, 12444-12459.
20. T. A. A. Oliver, Y. Zhang, M. N. R. Ashfold and S. E. Bradforth, *Faraday Discuss.* , 2011, **150**, 439-458.
21. Y. Zhang, T. A. A. Oliver, S. Das, A. Roy, M. N. R. Ashfold and S. E. Bradforth, *J. Phys. Chem. A*, 2013, **117**, 12125-12137.
22. Y. Zhang, T. A. A. Oliver, M. N. R. Ashfold and S. E. Bradforth, *Faraday Discuss.*, 2012, **157**, 141-163.
23. T. Posner, *Ber. Dtsch. Chem. Ges.*, 1905, **38**, 646-657.

24. O. Ito, *Res. Chem. Intermed.*, 1995, **21**, 69-93.
25. X. Zhang, N. Zhang, H. Schuchmann and C. Sonntag, *J. Phys. Chem.*, 1994, **98**, 6541-6547.
26. O. Ito, K. Nogami and M. Matsuda, *J. Phys. Chem.*, 1981, **85**, 1365-1368.
27. O. Ito and M. Matsuda, *J. Am. Chem. Soc.*, 1979, **101**, 1815-1819.
28. G. M. Roberts, H. J. B. Marroux, M. P. Grubb, M. N. R. Ashfold and A. J. Orr-Ewing, *J. Phys. Chem. A*, 2014, **118**, 11211-11225.
29. M. J. Frisch, G. W. Trucks, H. B. Schlegel, G. E. Scuseria, M. A. Robb, J. R. Cheeseman, G. Scalmani, V. Barone, B. Mennucci, G. A. Petersson et al. *Gaussian 09, Revision B.01,* Gaussian Inc., Wallingford CT, 2009.
30. C. Lee, W. Yang and R. G. Parr, *Phys. Rev. B*, 1988, **37**, 785-789.
31. A. D. Becke, *J. Chem. Phys.*, 1993, **98**, 5648-5652.
32. H.-J. Werner, P. J. Knowles, G. Knizia, F. R. Manby, M. Schütz, P. Celani, T. Korona, R. Lindh, A. Mitrushenkov, G. Rauhut et al. *MOLPRO, version 2010.1, A Package of Ab Initio Programs,* 2010.
33. T. H. J. Dunning, *J. Chem. Phys.*, 1989, **90**, 1007-1023.
34. D. E. Woon and T. H. J. Dunning, *J. Chem. Phys.*, 1993, **98**, 1358-1371.
35. R. Hermann, G. R. Dey, S. Naumovc and O. Brede, *Phys. Chem. Chem. Phys.*, 2000, **2**, 1213-1220.
36. Y. M. Riyad, S. Naumov, R. Hermann and O. Brede, *Phys. Chem. Chem. Phys.*, 2006, **8**, 1697-1706.
37. M. P. Grubb, A. J. Orr-Ewing and M. N. R. Ashfold, *Rev. Sci. Instrum*, 2014, **84**, 064104.
38. H. Masuhara, H. Miyasaka, N. Ikeda and N. Mataga, *Chem. Phys. Lett.*, 1981, **82**, 59-62.
39. Y. Hirata, Y. Niga and T. Okada, *Chem. Phys. Lett.*, 1994, **221**, 283-288.
40. N. A. Borisevich, Y. N. Malkin, S. Ruziev, S. V. Mel'nichuk, S. A. Tikhomirov, S. A. Tolstorozhev and V. A. Kuz'min, *Bull. Acad. Sci. USSR, Div. Chem. Sci.*, 1990, **39**, 468-471.
41. K. Griesbaum, *Angew. Chem., Int. Ed. Engl*, 1970, **9**, 273-287.
42. J. A. Howard in *Free Radicals,* ed. J. K. Kochi, Wiley, New York, 1973, vol. 11, pp. 1.
43. *Ullmann's Encyclopedia of Industrial Chemistry 6th Edn.* Wiley-VCH, Weinheim 1998, vol. 34, pp. 384.

Table of Contents Graphic

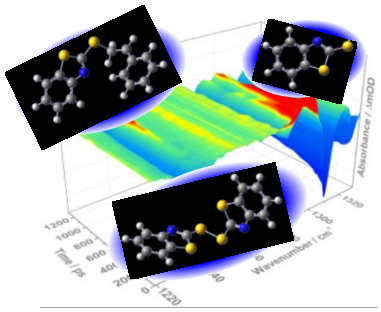

A carbon-centered intermediate radical of a thiol-ene reaction is directly probed on the picosecond time scale with time-resolved vibrational absorption spectroscopy.